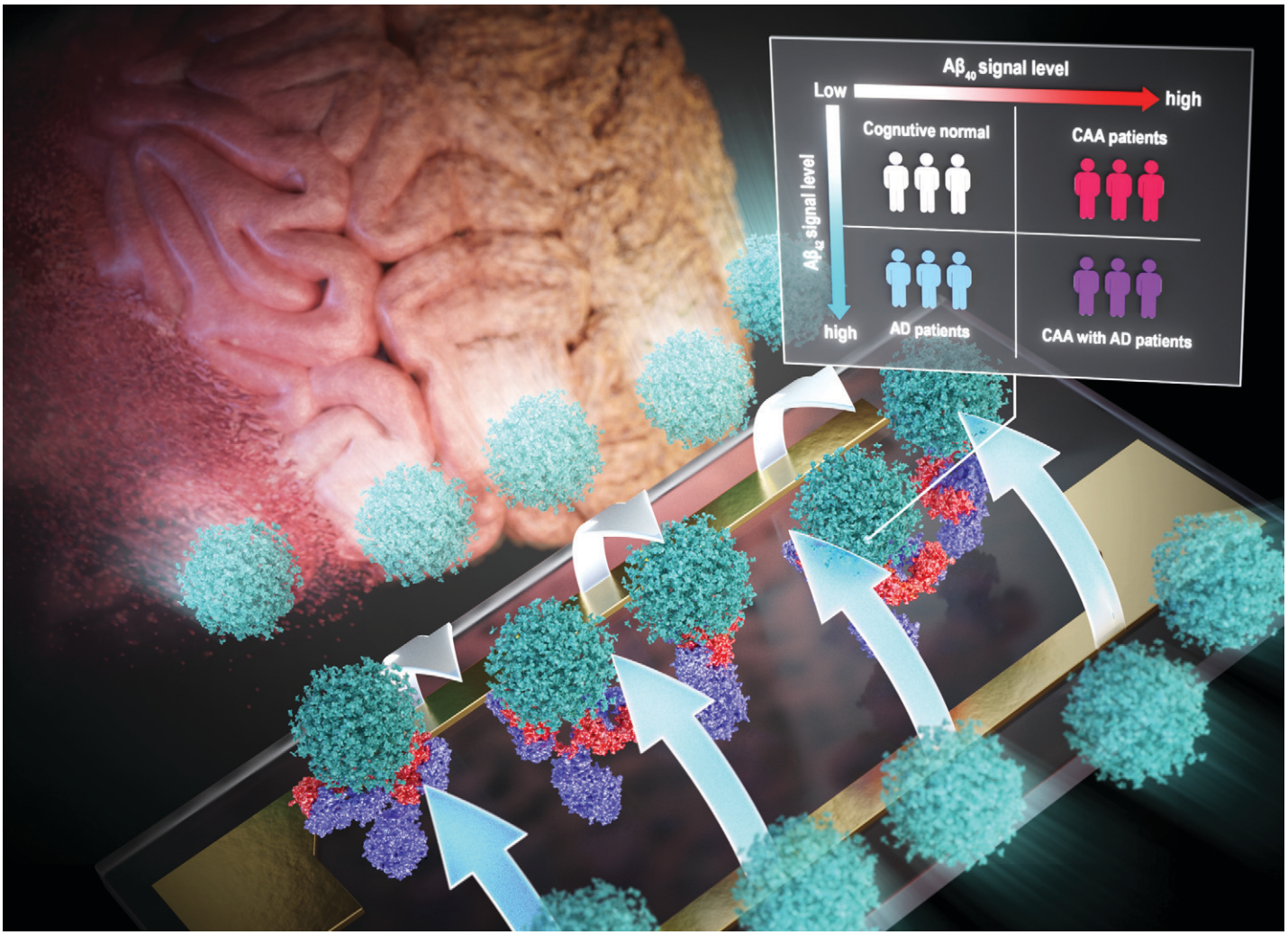

Featuring work from the Advanced Precision Medicine Laboratory of Professor Kyo Seon Hwang and Professor Jin San Lee, College of Medicine, Kyung Hee University, Seoul, Republic of Korea.

Screening for cerebral amyloid angiopathy based on serological biomarkers analysis using a dielectrophoretic force-driven biosensor platform

A highly sensitive dielectrophoretic-driven biosensor platform allows accurate screening of cerebral amyloid angiopathy, which may give rise to cerebral hemorrhage and Alzheimer's disease, by simple blood tests.

As featured in:

See Jin San Lee, Kyo Seon Hwang *et al.*, *Lab Chip*, 2021, **21**, 4557.

ROYAL SOCIETY OF CHEMISTRY

rsc.li/loc

Registered charity number: 207890

Lab on a Chip

PAPER

View Article Online
View Journal | View Issue

Cite this: *Lab Chip*, 2021, **21**, 4557

Screening for cerebral amyloid angiopathy based on serological biomarkers analysis using a dielectrophoretic force-driven biosensor platform†

Hye Jin Kim,[a] Dongsung Park,[a] Gyihyaon Yun,[b] Hongrae Kim,[a] Hyug-Gi Kim,[c] Kyung Mi Lee,[c] Il Ki Hong,[d] Key-Chung Park,[e] Jin San Lee*[e] and Kyo Seon Hwang*[a]

We aimed to analyze plasma amyloid-β (Aβ)$_{1–40}$ and Aβ$_{1–42}$ using a highly sensitive dielectrophoretic-driven biosensor platform to demonstrate the possibility of precise cerebral amyloid angiopathy (CAA) diagnosis in participants classified according to Aβ-positron emission tomography (PET) positivity and the neuroimaging criteria for CAA. We prospectively recruited 25 people with non-Alzheimer's disease (non-AD) and 19 patients with Alzheimer's disease (AD), which were further classified into the CAA− and CAA+ (possible and probable CAA) groups according to the modified Boston criteria. Patients underwent plasma Aβ analysis using a highly sensitive nano-biosensor platform, Aβ-PET scanning, and detailed neuropsychological testing. As a result, the average signal levels of Aβ$_{1–42/1–40}$ differed significantly between the non-AD and AD groups, and the CAA+ group exhibited significantly higher Aβ$_{1–40}$ signal levels than the CAA− group in both non-AD and AD groups. The concordance between the Aβ$_{1–40}$ signal level and the neuroimaging criteria for CAA was nearly perfect, with areas under the curve of 0.954 (95% confidence interval (CI) 0.856–1.000), 0.969 (0.894–1.000), 0.867 (0.648–1.000), and 1.000 (1.000–1.000) in the non-AD/CAA− *vs.* non-AD/possible CAA, non-AD/CAA− *vs.* non-AD/probable CAA, AD/CAA− *vs.* AD/possible CAA, and AD/CAA− *vs.* AD/probable CAA groups, respectively. Higher Aβ$_{1–40}$ signal levels were significantly associated with the presence of CAA according to regression analyses, and the neuroimaging pattern analysis partly supported this result. Our findings suggest that measuring plasma Aβ$_{1–40}$ signal levels using a highly sensitive biosensor platform could be a useful non-invasive CAA diagnostic method.

Received 20th August 2021,
Accepted 25th October 2021

DOI: 10.1039/d1lc00742d

rsc.li/loc

1. Introduction

Cerebral amyloid angiopathy (CAA) is a cerebrovascular disease caused by the accumulation of vascular amyloid-β (Aβ) in the tunica media and adventitia of cortical and leptomeningeal small vessels. It is a major cause of spontaneous lobar intracranial hemorrhage (ICH) and an important contributor to dementia in older people.[1] Further, CAA is a common, degenerative, small vessel disease of the brain in older individuals and is a prominent comorbidity of Alzheimer's disease (AD) that exacerbates vascular cognitive impairment. Population-based neuropathological studies have reported CAA prevalence of 50–60% and 20–40% in older populations with and without dementia, respectively.[2] Specifically, up to 85% of patients with AD have CAA pathology.[1,3] CAA is independently associated with cognitive impairment and dementia, even after controlling for AD.[3–5] However, the interaction of detrimental effects between CAA and AD on global cognition has also been demonstrated. Patients with both CAA and AD exhibited significantly worse neuropsychological performance than those with AD alone, even after adjusting for potential confounders.[2,6] Thus, there is growing interest in the early detection of CAA, given its association with AD and cerebrovascular disease in older individuals. Additionally, because there is no disease-

[a] *Department of Clinical Pharmacology and Therapeutics, College of Medicine, Kyung Hee University, Seoul 02447, Republic of Korea. E-mail: k.hwang@khu.ac.kr; Tel: +82 2 961 9676*
[b] *Department of Medicine, Graduate School, Kyung Hee University, Seoul 02447, Republic of Korea*
[c] *Department of Radiology, Kyung Hee University Hospital, College of Medicine, Kyung Hee University, Seoul 02447, Republic of Korea*
[d] *Department of Nuclear Medicine, Kyung Hee University Hospital, College of Medicine, Kyung Hee University, Seoul 02447, Republic of Korea*
[e] *Department of Neurology, Kyung Hee University Hospital, College of Medicine, Kyung Hee University, Seoul 02447, Republic of Korea. E-mail: xpist@naver.com; Tel: +82 2 958 8499*

† Electronic supplementary information (ESI) available. See DOI: 10.1039/d1lc00742d

modifying treatment for CAA to date, early detection and optimization of treatment of CAA are essential for patients with unusual situations, such as those on antithrombotics, with coexisting AD or those with the apolipoprotein E (APOE) ε2 allele (for hematoma expansion in CAA). To diagnose the CAA, the modified Boston criteria using MRI is being utilized, and it has been confirmed that 90% of patients with neuroimaging-diagnosed CAA have moderate-to-severe CAA upon neuropathology.[1] Non-invasive neuroimaging criteria for CAA have been established using blood-sensitive MRI sequences, which focus on the presence of hemorrhagic manifestations of CAA: lobar cerebral microbleeds (CMBs) and cortical superficial siderosis (cSS).[7] However, a definite CAA diagnosis can be made only after a postmortem pathological examination of the brain.

Decreased levels of cerebrospinal fluid (CSF) $A\beta_{1-40}$ and $A\beta_{1-42}$ have been reported in patients with CAA, which may be explained by impaired Aβ clearance from interstitial cerebral fluid in CAA.[8–10] Moreover, as $A\beta_{1-40}$ peptides are the predominant forms of Aβ deposited in the vessel walls of arteries and veins in CAA, there have been many efforts to detect $A\beta_{1-40}$ in the blood for CAA diagnosis. However, in contrast to CSF biomarkers for CAA, the correlation between plasma Aβ levels and the presence of CAA remains controversial.[2,6] Nevertheless, considering the advantages in terms of cost, non-invasiveness, and repeated measurement ability, there is a need to develop blood-based CAA biomarkers. The major challenge in the development of blood-based CAA biomarkers is the selective analysis of extremely low levels of $A\beta_{1-40}$ and $A\beta_{1-42}$ (approximately pg mL^{-1}) in the blood.[7] This requires a biosensing platform with high selectivity and sensitivity. In our previous study, we developed a sensing platform capable of analyzing biomolecules at levels in the range of fg mL^{-1} with high accuracy.[11,12] Our biosensor platform is manufactured *via* micro/nano-fabrication technology and detects changes in electrical signals, particularly impedance change, to quantify a few fg mL^{-1} of biomolecules. In particular, unlike conventional sensing platforms, our platform includes the use of dielectrophoresis (DEP), which enriches biomolecules present at extremely low levels in the plasma, making high-sensitivity/high-precision plasma-based biomolecule analysis possible.

Here, we report the possibility of precise CAA screening by analyzing plasma Aβ using a highly sensitive biosensor platform fabricated by combing micro/nanotechnology with DEP in participants classified according to Aβ-PET positivity and neuroimaging criteria for CAA. First, we demonstrated that the plasma $A\beta_{1-42/1-40}$ ratio was an excellent predictor of Aβ-PET positivity, suggesting that our method is reliable for the selective analysis of extremely low levels of plasma $A\beta_{1-40}$ and $A\beta_{1-42}$. Also, it was confirmed that in participants with CAA, the average plasma $A\beta_{1-40}$ signal levels were statistically significantly higher than in participants without CAA in both the non-AD and AD groups. Moreover, when participants with CAA were classified according to the neuroimaging criteria for CAA, plasma $A\beta_{1-40}$ levels were higher in participants with probable CAA than in those with possible CAA or without CAA in both groups. Higher levels of plasma $A\beta_{1-40}$ were also significantly associated with the presence of CAA, and the neuroimaging pattern analysis partly supported this result.

Experimental

Reagents and materials

Sulfuric acid (H_2SO_4, 98%), hydrogen peroxide (H_2O_2, 35%), and isopropyl alcohol (IPA, 99.7%) were purchased from Daejung Chemical & Metals Co. Ltd., (Gyeonggi-do, Korea). 3-(Ethoxydimethylsilyl) propylamine (APMES, 97%), *N*-(3-dimethyl aminopropyl)-*N*-ethylcarbodiimide hydrochloride (EDC, molecular weight [MW]: 155.249 g mol^{-1}), *N*-hydroxysuccinimide (NHs, MW: 115.09 g mol^{-1}), and glutaraldehyde solution (50 wt%) were purchased from Sigma-Aldrich Inc. (St. Louis, MO, USA). We purchased 100 mM phosphate-buffered saline (PBS, pH 7.4) from Corning Korea Co. Ltd., (Seoul, Korea) and 0.2 M 2-morpholinoethanesulfonic acid monohydrate (MES, pH 5.5) buffer from Thermo Fisher Scientific Ltd. (Waltham, MA, USA). Standard plasma was purchased from Sigma-Aldrich Inc. (St Louis, MO, USA). Polydimethylsiloxane (SYLGARD 184 A/B) was purchased from Dowhitech Silicone Co. Ltd. (Gyeonggi-do, Korea). All reagents and solvents were used as received without further purification. The distilled water (DW) used in all experiments had a resistivity higher than 18 MΩ cm^{-1} from the AquaMAX™ Ultra 370 series (Young In Chromass Co., Gyeonggi-do, Korea). Amyloid-β (Aβ) protein fragments 1–40 ($A\beta_{1-40}$) and 1–42 ($A\beta_{1-42}$), with an MW of approximately 4.5 kilodalton (kDa), and human hemoglobin were purchased from Sigma-Aldrich Inc. Purified anti-Aβ, 1–40 (11A50–B10) antibody, and purified anti-Aβ, 1–42 (12F4) antibody, which were specific for the isoform ending at the 40th and 42nd amino acids of Aβ, respectively, were purchased from BioLegend Inc. (San Diego, CA, USA).

Clinical study participants

Written informed consent was obtained from all participants before inclusion in the study. The study was approved by the Institutional Review Board (IRB) of Kyung Hee University Hospital (IRB No. 2018-01-023). We prospectively recruited 44 individuals who underwent plasma Aβ analysis, high-resolution 3 T brain MRI, 18F-florbetaben PET, and detailed neuropsychological testing.[8] The patients comprised 20 cognitively normal individuals, 7 patients with amnestic mild cognitive impairment (aMCI), and 17 with probable Alzheimer's disease (AD) dementia, all of whom had been clinically diagnosed at the Memory Disorders Clinic of Kyung Hee University Hospital (Seoul, Korea) from December 2018 to September 2019. Cognitively normal individuals had no objective cognitive dysfunction in any cognitive domain in the detailed neuropsychological tests. Patients with aMCI were diagnosed according to the Petersen criteria,[9] with modifications that have been described in detail elsewhere.[10]

Patients with probable AD dementia fulfilled the criteria proposed by the National Institute of Neurological and Communicative Disorders and Stroke and the AD and Related Disorders Association.[14] Brain MRI confirmed the absence of structural lesions, including cerebral hemorrhage or infarction, hippocampal sclerosis, brain tumors, traumatic encephalomalacia, and vascular malformation. The exclusion criteria included a history of psychological disease, stroke, brain surgery, seizure, head trauma, severe cerebral white matter hyperintensities defined by the modified Fazekas scale,[10] or current systemic medical diseases that could affect cognition.

Laboratory tests were conducted for all participants to rule out other causes of cognitive impairment. These tests included complete blood counts, vitamin B12 levels, folate levels, metabolite profiles, thyroid function tests, and syphilis serology. Genomic DNA was extracted from whole blood samples to perform apolipoprotein E (APOE) genotyping according to the manufacturer's instructions (QIAGEN GmbH, Hilden, Germany).

Plasma acquisition and sampling protocol

Approximately 10 mL of blood was drawn from each participant using a heparin vacutainer tube (sodium heparin vacutainer, BD, Franklin Lakes, NJ, USA). The tube was gently shaken to mix the blood and anticoagulant sufficiently. The sample was centrifuged at 3000 rpm at 4 °C for 15 min, and the supernatant (approximately 4–5 mL) was transferred into a 1.5 mL polypropylene (PP) tube to separate the plasma. Then, 1× protease inhibitor (version 09, complete mini-ethylenediaminetetraacetic acid-free) in 10 mM phosphate-buffered saline (PBS) was added to the supernatant, and the samples were gently mixed for 30–60 s. Finally, the plasma was carefully transferred into a fresh 1.5 mL PP tube and stored at −80 °C.

Brain MRI system set-up

Structural 3-dimensional (3D) T1-weighted images (T1WIs) were acquired using a 3.0 T MR system (Achieva TX, Philips Medical Systems, Best, The Netherlands) equipped with a 32-channel sensitivity-encoding head coil and multi-transmit technology. The T1WI sequence used was a magnetization-prepared rapid-acquisition gradient-echo sequence with the following parameters: relaxation time = 9.0 ms, echo time = 5.0 ms, flip angle = 8°, field-of-view = 256 × 256 mm^3, and voxel size = 1 × 1 × 1 mm^3.

Assessment of cerebral amyloid angiopathy (CAA) imaging markers

Lobar cerebral microbleeds were defined as microbleeds located in lobar areas and meeting the following consensus criteria:[2] (1) homogeneous signal losses with blooming effects on T2* images, (2) round or ovoid lesions with a 10 mm diameter cut-off, (3) lesions surrounded at least half by brain parenchyma, and (4) distinct from other potential mimics, such as iron or calcium deposits, or vessel flow voids. Cortical superficial siderosis (cSS) was defined as chronic blood residual products in superficial layers of the cerebral cortex or subarachnoid area, with the following guidelines:[15] (1) bilinear track-like hypointensities on T2* images surrounding or within a cerebral sulcus; (2) absence of corresponding hyperintense signals on FLAIR images; (3) supratentorial location; and (4) exclusion of a previous ICH-associated cSS. Participants were included in the CAA+ group if they fulfilled at least the criteria for possible CAA according to the modified Boston criteria.[15] In the current study, the CAA+ group consisted of 20 participants, among whom 10 met the neuroimaging criteria for probable CAA.

^{18}F-florbetaben PET/computed tomography acquisition for participant classification *via* neuroimaging analysis

3D static PET images were acquired 90 min after intravenously injecting 296 MBq of ^{18}F-florbetaben using a Gemini TF 16 PET/computed tomography (CT) scanner (Philips Healthcare, Cleveland, OH, USA). CT images were acquired from the vertex to the skull base (50 mAs; 120 kVp; slice 2 mm), and 10 mm PET images were immediately acquired over the same region. We used the ordered-subset expectation-maximization algorithm (iteration = 3 and subset = 33) to reconstruct 3D PET images in a 128 × 128 × 20 matrix with a voxel size of 2 × 2 × 2 mm^3.

All Aβ-PET images were visually assessed and dichotomized as Aβ-positive or Aβ-negative after being reviewed by nuclear medicine physicians who were blinded to the participants' information. Aβ-PET findings were considered positive when the brain amyloid-plaque load (BAPL) score was 2–3 based on visual assessment.[16] Regarding regional cortical tracer uptake (RCTU), image evaluators used the RCTU scoring system (RCTU 1, no tracer uptake; RCTU 2, moderate tracer uptake; and RCTU 3, pronounced tracer uptake) in the lateral temporal cortex, frontal cortex, posterior cingulate cortex/precuneus, and parietal cortex. In terms of RCTU and BAPL correspondence, an RCTU score of 1 in each brain region was considered to be identical to a BAPL score of 1. An RCTU score of 2 in at least one brain region and no score of 3 was considered to be equivalent to a BAPL score of 2. An RCTU score of 3 in any of the four brain regions was considered to be a BAPL score of 3. Aβ-negative status was given to participants with a BAPL score of 1, while Aβ-positive status was given to those with BAPL scores of 2–3.

We also conducted a quantitative Aβ-PET analysis using the cortical standardized uptake value ratio (SUVR) in all PET scans. Based on a previous study,[17] an SUVR cut-off of ≥1.43 was selected as the amyloid-positivity criterion. In this study, our visual assessment strongly corresponded with the binarized global ^{18}F-florbetaben PET binding evaluations, as the comparison of the two methods resulted in high accuracy of 100% (25 participants were Aβ-negative [20 normal individuals and five patients with aMCI] and 19 were Aβ-positive [two patients with aMCI and 17 with AD dementia]).

Pattern analysis of Aβ accumulation in the brain

Pattern analysis was performed with MRI and Aβ-PET images to estimate the relative levels of plasma $A\beta_{1-40}$ and $A\beta_{1-42}$ in the brain visually. First, cortical and subcortical brain regions were automatically segmented using Freesurfer 5.3 (http://surfer.nmr.mgh.harvard.edu/), following the pipeline described in https://surfer.nmr.mgh.harvard.edu/fswiki/recon-all. Second, ^{18}F-florbetaben PET images were co-registered to the 3D T1WI-labeled data using the Statistical Parametric Mapping version 12 program (Wellcome Department of Imaging Neuroscience, University College, London, UK). Amyloid cortical SUVR was determined as the average of the standardized uptake value normalized by the uptake in the cerebellar gray matter, with this reference region being selected from the cerebellum external and cortex segments on MRI. Third, pattern analysis was conducted between Aβ present in the plasma and SUVR in Aβ-PET using the coefficient of linear correlation. The results show the average correlation coefficient in each brain region of interest as color-coded overlays on the representative MRI.

Fabrication of the sensing platform and surface activation

Our biosensing platform consists of six interdigitated microelectrodes (IMEs), with a single IMEs having 30 pairs of interdigitated electrodes with a spacing and width of 5 μm and length of 300 μm. The platform was fabricated through a standard microelectromechanical systems process, as shown in Fig. S1:†[11] Silicon dioxide (SiO_2) and 300/1500 Å tantalum/platinum (Ta/Pt) layers were sequentially deposited on a cleaned 4 inch silicon wafer through thermal oxidation and sputtering processes, respectively. Subsequently, interdigitated micropatterns were drawn on the Ta/Pt surface with photoresist (PR) *via* a photolithography process, and the Ta/Pt layer was etched using an inductively coupled plasma etching process. Finally, the PR patterns were stripped, and a 4 inch wafer was scribed through the dicing process.

Then, IMEs were subjected to surface treatment processes to immobilize two types of antibodies (11A50–B10 and 12F4, referred to as $A\beta_{1-40}$-specific antibodies and $A\beta_{1-42}$-specific antibodies, respectively) on a SiO_2 surface between the electrodes of the sensor.[11] First, the surface was sequentially cleaned with piranha solution ($H_2SO_4 : H_2O_2$ (v/v) = 4 : 1), DW, and IPA. Then, a self-assembled monolayer was coated onto the SiO_2 surface by exposing the surface to 1% (w/v) APMES vapor for 5 min at 80 °C and stabilizing the surface for 20 min at room temperature (RT). After activating the surface with APMES, the surface was treated with a crosslinking solution obtained by mixing 50 mM EDC and 190 mM NHS in 0.2 M MES buffer for 1 h at 37 °C. Finally, the antibody solution diluted with 10 μg mL^{-1} in 10 mM PBS was immobilized on the surface of the sensor for 1 h at 37 °C. After immobilizing the antibodies on the sensing platform, a micro-fluidic channel was attached to the sensor's surface *via* Van der Waals force, and a 1% (v/v) hemoglobin solution in DW was injected into the channel for 1 h at RT to minimize non-specific adsorption occurring on the sensor and fluidic channel surfaces.

Immunoassay and signal analysis

To apply DEP force during the reaction of the Aβ to the antibodies immobilized on the biosensor surface, an alternating current voltage was generated using a DG4062 series waveform generator (Rigol Technologies Inc., Beaverton, OR, USA) and applied to the sensor for 20 min (Fig. S2†). Unbound Aβs were washed away using 1 mM PBS. The intensity and frequency of the applied alternating (AC) voltage were set to 0.5 V and 100 MHz, respectively, based on our previous results.[12]

The electrical signal of the sensor was measured at 1 kHz for 3 min (Fig. S3 and S4†) using an impedance analyzer (Cantis Inc., Gyeonggi-do, Korea). The values measured for 30 s after signal saturation were averaged and used as the output signal of the sensor. Specific binding between the Aβs and antibodies immobilized on the surface of the sensor was analyzed by calculating the difference in the electrical signal (ΔZ) before and after binding of the Aβs as follows:

$$|\Delta Z|(\%) = \frac{|Z_{\text{after}}| - |Z_{\text{before}}|}{|Z_{\text{before}}|} \times 100 \quad (1)$$

where Z_{before} and Z_{after} refer to the average electrical signals measured before and after the antibody–Aβs reactions, respectively (Table S1†).

Statistical analyses

Continuous variables were compared using Student's *t*-test and are presented as mean ± standard deviation (SD). Categorical variables were compared using the chi-square test or Fisher's exact test. For multiple comparisons, we performed non-parametric statistical testing as the data were not normally distributed (Kruskal–Wallis one-way analysis of variance [ANOVA] with the Dunn test for *post hoc* comparison between individual pairs). Univariate logistic regression analyses were performed to determine whether higher levels of plasma Aβ and Aβ-PET SUVR were associated with the presence of CAA. Since age, history of hypertension, and APOE ε4 are well known, strong risk factors for CAA,[8] we performed multivariate logistic regression analyses after adjusting for these variables in model 1 (age and history of hypertension) and model 2 (further adjusted for APOE ε4 status). Statistical significance was set at $p < 0.05$ in two-tailed tests. Statistical analyses were performed using SPSS (version 20.0; SPSS Inc., Chicago, IL, USA) and Prism 8 GraphPad (San Diego, USA).

Results

Excellent performance of platform in plasma-based Aβ analysis

As $A\beta_{1-40}$ is the main vascular Aβ involved in the pathogenesis of CAA and $A\beta_{1-42}$ is mainly a parenchymal Aβ involved in the development of AD,[1] we hypothesized that the

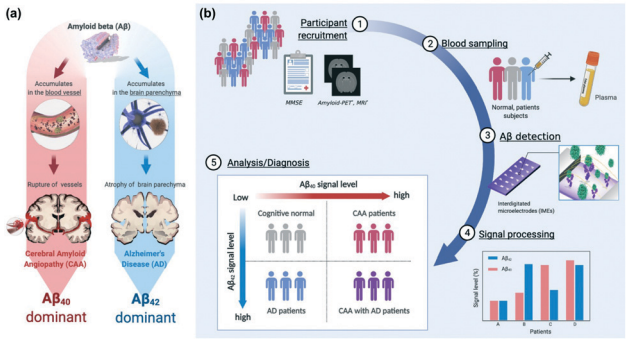

Fig. 1 Screening of Alzheimer's disease (AD) and cerebral amyloid angiopathy (CAA) by analyzing two species of amyloid beta (Aβ) with the highly sensitive sensing platform. (a) Pathogenesis of AD and CAA. (b) Schematic illustration for CAA and AD diagnosis using the highly sensitive Aβ sensors.

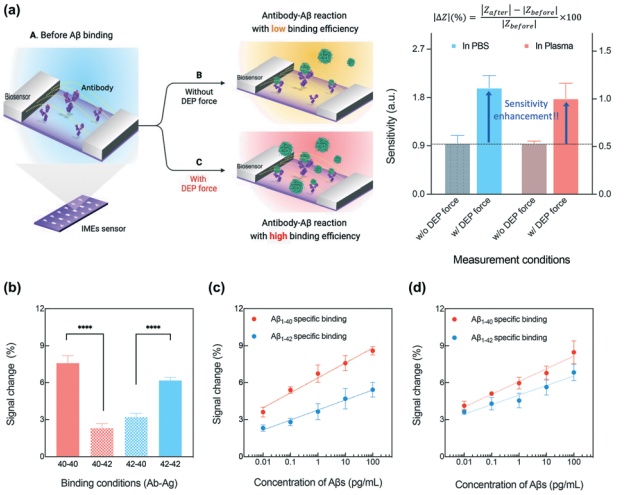

Fig. 2 High performance of dielectrophoretic (DEP) force-driven sensing platform. (a) Schematic diagram of sensor performance enhancement by DEP force. (b) Highly sensitive plasma-based analysis of Aβ for each specific antibody (12F4 and 11A50–B10). Excellent sensitivity of the biosensor for Aβ analysis in (c) PBS and (d) standard plasma. Error bars represent ± standard deviation (n = 18), and p-values are indicated with asterisks: *$p < 0.05$, **$p < 0.01$, ***$p < 0.001$, ****$p < 0.0001$. Aβ = amyloid-β; AD = Alzheimer's disease; CAA = cerebral amyloid angiopathy; PBS = phosphate buffered saline.

plasma signal level of $A\beta_{1-40}$, rather than that of $A\beta_{1-42}$, would be higher in participants with CAA than in those without CAA, whereas the plasma signal level of $A\beta_{1-42}$ would be higher than that of $A\beta_{1-40}$, in participants with AD than in those without AD (Fig. 1). To prove our hypothesis, we developed a highly sensitive and selective biosensing platform based on DEP forces which manipulates biomolecules in a non-uniform electric field (E-field) region depending on the applied intensity and the frequency of alternating current (AC) voltage.[13] Especially, according to the applied frequency, two types of DEP forces can occur depending on the applied frequency – a positive force that attracts biomolecules into the dense E-field region while a negative force that pushes them out of the dense region.[13] Of these two types, the negative type was used to improve the electrical signal change of the sensor by enriching Aβs on the surface between electrodes to which their specific antibodies were immobilized (*i.e.*, the Aβ response region). Consequently, the binding efficiency was enhanced approximately 2-folds by the DEP force[12] (Fig. 2a).

The specificity of our biosensor was demonstrated by comparing the signals that occurred when $A\beta_{1-40}$ and $A\beta_{1-42}$ reacted to both types of immobilized antibodies (Fig. 2b). In the biosensor in which $A\beta_{1-40}$-specific antibodies were immobilized, a higher signal change occurred following the binding of $A\beta_{1-40}$ compared with the change following the binding of $A\beta_{1-42}$ (approximately 7.583 ± 0.607% *vs.* 2.165 ± 0.394%, respectively; $p < 0.0001$), whereas in the biosensor where $A\beta_{1-42}$-specific antibodies were immobilized, the signal change owing to the binding of $A\beta_{1-42}$ was higher than that owing to binding of $A\beta_{1-40}$ (approximately 5.928 ± 0.357% *vs.* 3.183 ± 0.318%, respectively; $p < 0.0001$). The noise level was approximately 2.086 ± 0.585%, which is indicated by the gray column in Fig. S5.†

Then, the sensitivity of the sensor was confirmed by linear regression analysis of the impedance change according to the concentration of Aβs (linear equation: y = intercept + slope·x, the value of the slope signifies the sensitivity of the biosensor for Aβ binding) in two physiological buffers (1 mM PBS and standard plasma). The changes by the specific binding of $A\beta_{1-40}$ and $A\beta_{1-42}$ in the 1 mM PBS ranged from approximately 3.609 ± 0.401% to 8.599 ± 0.345% and from 2.31 ± 0.260 to 5.43 ± 0.603%, depending on the concentration of the Aβs, respectively (Fig. 2c). Based on these changes, the sensitivity of the sensor (namely, the slope of the linear fitting line in the figure) was calculated to be approximately 1.216 ± 0.053 and 0.8138 ± 0.107 for $A\beta_{1-40}$ and $A\beta_{1-42}$ detection, respectively. Also, changes due to the specific binding of $A\beta_{1-40}$ and $A\beta_{1-42}$ spiked in the standard plasma, ranging from approximately 4.126 ± 0.369% to 8.476 ± 0.935% and from 3.627 ± 0.201% to 6.836 ± 0.657%, respectively, depending on the level of Aβs (Fig. 2d), and the sensitivities were verified to be approximately 1.036 ± 0.091 and 0.777 ± 0.106 for $A\beta_{1-40}$ and $A\beta_{1-42}$ detection, respectively. The detailed values are described in Table S1,† and these results collectively demonstrated the excellent sensitivity and specificity of our biosensing platform in the Aβ assay.

Differential diagnosis of CAA in each group using the highly sensitive biosensing platform

Based on Aβ-PET positivity, participants were classified into the non-AD (n = 25) and AD (n = 19) groups, and the average signal levels of $A\beta_{1-40}$ and $A\beta_{1-42}$ were significantly different in the two groups (Table S2†).

This difference between the two groups was clearly reduced when the signal level of $A\beta_{1-42}$ was divided by that of $A\beta_{1-40}$ (non-AD *vs.* AD: $p < 0.001$, $p < 0.01$, and $p < 0.01$ for $A\beta_{1-42/1-40}$, $A\beta_{1-40}$, and $A\beta_{1-42}$, respectively; t-test) (Fig. 3a and S6†). The participants with $A\beta_{1-42/1-40}$ signal levels exceeding 1.016 were considered as AD patients, as this value produced

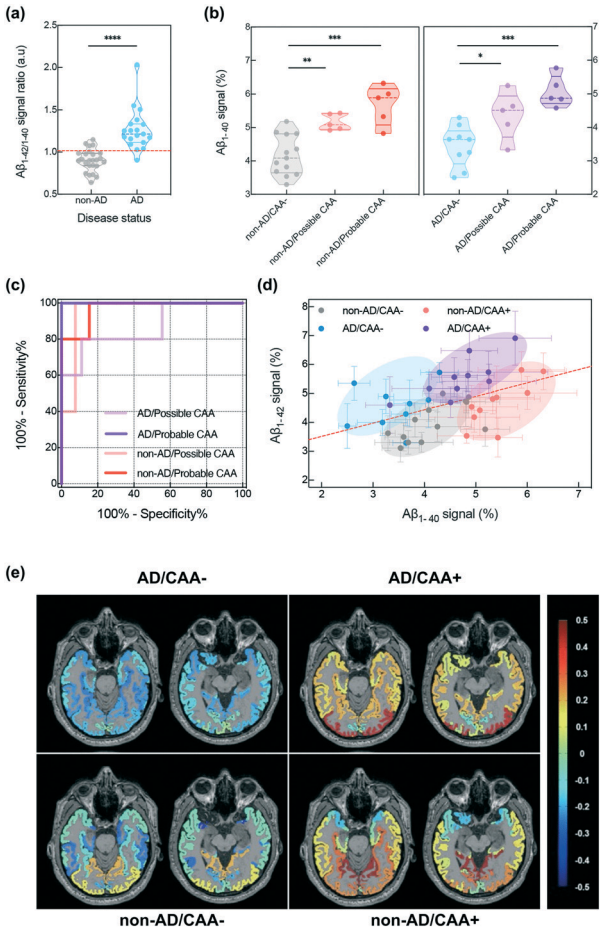

Fig. 3 Screening of CAA in the non-AD and AD groups based on the analysis of plasma $A\beta_{1-42}$ and $A\beta_{1-40}$ levels. To distinguish between the non-AD and AD groups, the relative signal level of $A\beta_{1-42}$ and $A\beta_{1-40}$ is calculated. (a) The ratio of the signal between the $A\beta_{1-42}$ and $A\beta_{1-40}$ is higher in the AD group than in the non-AD group. (b) The signal level of $A\beta_{1-40}$ and ROC analysis in the non-AD/CAA− *vs.* non-AD/possible CAA (light purple line), non-AD/CAA− *vs.* non-AD/probable CAA (purple line), AD/CAA− *vs.* AD/possible CAA (light red line), and AD/CAA− *vs.* AD/probable CAA groups (red line). (c) The AUC values that were calculated by using the ROC are 0.954 (95% CI 0.856–1.000), 0.969 (95% CI 0.894–1.000), 0.867 (95% CI 0.648–1.000), and 1.000 (95% CI 1.000–1.000) in the non-AD/CAA− *vs.* non-AD/possible CAA, non-AD/CAA− *vs.* non-AD/probable CAA, AD/CAA− *vs.* AD/possible CAA, and AD/CAA− *vs.* AD/probable CAA groups, respectively. (d) Non-AD/CAA−, non-AD/CAA+, AD/CAA−, and AD/CAA+ are diagnosed based on the signal level of plasma $A\beta_{1-40}$ and $A\beta_{1-42}$. (e) Correlation coefficient (r) between plasma $A\beta_{1-40}$ and Aβ-PET SUVRs on representative T1-weighted MRI using pattern analysis in the non-AD/CAA−, non-AD/CAA+, AD/CAA−, and AD/CAA+ groups. A moderate positive correlation (red color) is observed in the occipital cortex only in the CAA+ groups of non-AD/CAA+ and AD/CAA+. p-values are indicated with asterisks: $*p < 0.05$, $**p < 0.01$, $***p < 0.001$, $****p < 0.0001$. Aβ = amyloid-β; AD = Alzheimer's disease; AUC = area under curve; CAA = cerebral amyloid angiopathy; non-AD = non-Alzheimer's disease; ROC = receiver operating curve.

the maximum Youden Index with a positive percentage agreement of 0.81 (95% CI 0.75–0.99) and a negative percentage agreement of 0.95 (95% CI 0.65–0.93) with Aβ-PET positivity. Through a receiver operating characteristic curve analysis, the ratio of $A\beta_{1-42/1-40}$ has proved to be the best predictor of Aβ-PET positivity, and the area under the curve (AUC) was 0.952 (95% CI 0.89–1.00, Fig. S7†). We further subdivided the non-AD and AD groups according to the neuroimaging criteria for CAA into the CAA- and CAA+ groups. The non-AD/CAA+ and AD/CAA+ groups included 10 (40.0% of the non-AD group) and 10 (52.6% of the AD group) participants, respectively. The CAA+ groups were classified into possible and probable CAA groups according to the modified Boston criteria, and the participants were subdivided into six different groups: non-AD/CAA−, non-AD/possible CAA, non-AD/probable CAA, AD/CAA−, AD/possible CAA, and AD/probable CAA groups. Then, to verify the correlation between the neuroimaging criteria for CAA and plasma Aβ, the average $A\beta_{1-40}$ signal levels in the CAA subgroups were compared (Fig. 3b). The average $A\beta_{1-40}$ signal levels in the non-AD/possible CAA and non-AD/probable CAA groups were significantly higher than those in the non-AD/CAA− group ($p < 0.01$ in non-AD/CAA− *vs.* non-AD/possible CAA; $p < 0.001$ in non-AD/CAA− *vs.* non-AD/probable CAA; one-way ANOVA). Such an increase in $A\beta_{1-40}$ signal level was also consistent in the AD group ($p < 0.05$ in AD/CAA− *vs.* AD/possible CAA; $p < 0.001$ in AD/CAA− *vs.* AD/probable CAA; one-way ANOVA). The concordance between the $A\beta_{1-40}$ signal level and the neuroimaging criteria for CAA was nearly perfect, with AUCs of 0.954 (95% CI 0.856–1.000), 0.969 (95% CI 0.894–1.000), 0.867 (95% CI 0.648–1.000), and 1.000 (95% CI 1.000–1.000) in the non-AD/CAA− *vs.* non-AD/possible CAA, non-AD/CAA− *vs.* non-AD/probable CAA, AD/CAA− *vs.* AD/possible CAA, and AD/CAA− *vs.* AD/probable CAA groups, respectively (Fig. 3c). In contrast, the correlation between $A\beta_{1-42}$ signal level and the neuroimaging criteria for CAA was low (Fig. S8†).

Finally, we comprehensively analyzed the signals of $A\beta_{1-40}$ and $A\beta_{1-42}$ to confirm the possibility of discrimination between the non-AD/CAA−, non-AD/CAA+, AD/CAA−, and AD/CAA+ groups (Fig. 3d). Based on the linear regression curve showing the correlation between the $A\beta_{1-40}$ and $A\beta_{1-42}$ signal levels (slope = 0.461, correlation coefficient [r] = 0.52), most participants in the non-AD group were clustered under the regression curve, whereas most participants in the AD group were clustered over the curve. Moreover, regardless of the clustered regions above and below the regression curve, the CAA+ group had higher $A\beta_{1-40}$ signal levels than the CAA− group. Consequently, we confirmed that the non-AD/CAA−, non-AD/CAA+, AD/CAA−, and AD/CAA+ groups were successfully distinguished into four sectors of the graph. Further, images show the topographical pattern of r between plasma $A\beta_{1-42/1-40}$ signal level and Aβ-PET SUVRs (Fig. 3e). In the CAA+ groups, plasma $A\beta_{1-40}$ signal level and Aβ-PET SUVRs showed a moderate positive correlation in the occipital cortex suggesting participants with CAA had selectively higher neocortical Aβ deposition in that region. The results of binary logistic regression analyses for the presence of CAA according to plasma $A\beta_{1-40}$ signal level and Aβ-PET SUVR are presented in Table 1. Higher plasma $A\beta_{1-40}$ signal level (p = 0.003) and Aβ-PET SUVR (p = 0.032) were

Table 1 Association between the level of plasma $A\beta_{1-40}$, Aβ-PET SUVR, and presence of CAA

	Total presence of CAA		Non-AD presence of CAA		AD presence of CAA	
	B (SE)	*p*-value	B (SE)	*p*-value	B (SE)	*p*-value
$A\beta_{1-40}$						
Crude model	1.365 (0.459)	0.003	1.469 (0.651)	0.024	3.187 (1.382)	0.021
Model 1	1.198 (0.439)	0.006	1.109 (0.771)	0.150	3.203 (1.433)	0.025
Model 2	1.160 (0.468)	0.013	1.317 (0.859)	0.125	3.058 (1.426)	0.032
Aβ-PET SUVR						
Crude model	2.910 (1.354)	0.032	23.772 (10.872)	0.029	10.229 (4.899)	0.037
Model 1	2.500 (1.673)	0.135	25.734 (17.920)	1.151	11.198 (5.602)	0.046
Model 2	3.326 (1.871)	0.075	26.486 (19.538)	0.175	11.196 (5.889)	0.057

B (SE) = β value (standard error of the mean). Binary logistic analysis was performed to determine whether higher levels of plasma Aβ or Aβ-PET SUVR were associated with the presence of CAA. Model 1 was adjusted for age and history of hypertension. Model 2 was further adjusted for apolipoprotein E ε4 status. Non-AD = non-Alzheimer's disease; AD = Alzheimer's disease; Aβ = amyloid-β; PET = positron emission tomography; SUVR = standardized uptake value ratio.

significantly associated with the presence of CAA in study participants (crude model). Adjusting for the strong risk factors for CAA (age, history of hypertension, and APOE ε4 status) did not attenuate the association between plasma $A\beta_{1-40}$ signal level and presence of CAA, but it did attenuate the association with Aβ-PET SUVR. Additionally, in the non-AD group, higher plasma $A\beta_{1-40}$ signal level (p = 0.024) and Aβ-PET SUVR (p = 0.029) were significantly associated with the presence of CAA in the crude model only. In the AD group, higher plasma $A\beta_{1-40}$ signal level was significantly associated with the presence of CAA in the crude and adjusted models. However, the association between Aβ-PET SUVR and the presence of CAA was not statistically significant in model 2.

Discussion

In this study, we demonstrated that measuring plasma $A\beta_{1-40}$ signal level using a highly sensitive biosensor platform is feasible and could be a useful non-invasive method for screening CAA. We found a significant correlation between plasma $A\beta_{1-40}$ signal level and the presence of CAA. These findings are partly consistent with the results of a previous study that measured plasma Aβ levels using a commercial anti-Aβ assay kit in patients with CAA-related ICH and healthy controls.[18] Plasma $A\beta_{1-42}$ signal levels were higher in patients with probable CAA than in controls, and plasma $A\beta_{1-40}$ signal level was selectively elevated in patients with probable CAA compared with that in patients with possible CAA and healthy controls. Moreover, we found that participants had confirmed AD pathology and that plasma $A\beta_{1-42}$ levels were significantly different depending on the presence of CAA, even in the non-AD and AD groups. These results are significantly distinct from previous studies that reported that plasma $A\beta_{1-40}$ or $A\beta_{1-42}$ levels did not differ between patients with CAA-related ICH and healthy controls.[2] With the remarkable advances in neuroimaging of CAA using Aβ-PET, it has recently been demonstrated that vascular Aβ accumulation in CAA can be detected by quantifying Aβ-PET.[19] Comprehensive meta-analysis studies have reported that CAA participants without dementia had a higher global Aβ load than healthy controls.[19,20] Additionally, based on neuropathological studies reporting that the posterior region of the brain, particularly the occipital lobe, is severely affected by CAA,[21,22] most studies on Aβ-PET validity in CAA have demonstrated that patients with CAA have higher occipital-to-global Aβ ratios than those with AD.[1,19,20] Our results were consistent with the abovementioned findings: we identified significantly higher Aβ-PET SUVR values in participants with than in those without CAA. Furthermore, we confirmed that a higher plasma $A\beta_{1-40}$ level was significantly associated with the presence of CAA in the total population and particularly in those with AD pathology using models fully adjusted for the strong risk factors for CAA. Although we did not find statistical significance in the neuroimaging pattern analysis owing to the relatively small sample size, participants with CAA exhibited a moderate positive correlation between the levels of plasma $A\beta_{1-40}$ and Aβ-PET SUVRs in the occipital cortex in the non-AD and AD groups. Given that differentiating CAA from AD is challenging because Aβ-PET tracers label both parenchymal and vascular Aβ,[20] it is clear that our blood-based biosensor platform for CAA is a useful, cost-effective, and non-invasive screening method that reduces potential bias in the assessment of Aβ load. However, unfortunately, several limitations should be acknowledged before considering general clinical application of our findings. First, our study was conducted using blood samples collected from a cross-sectional study. Therefore, it was not possible to determine the temporal association between plasma Aβ levels and the presence of CAA, and further validation studies are needed. Second, because the sample size was small, particularly in terms of neuroimaging pattern analysis, the statistical power of our analyses was relatively low. Third, we did not evaluate other imaging markers (*e.g.*, white matter hyperintensities, enlarged perivascular spaces, and cortical microinfarcts) that may help diagnose CAA. Finally, our study participants were enrolled from a single memory clinic, which may limit the generalizability of these results. Therefore, we plan to more clearly demonstrate the possible relevance of plasma $A\beta_{1-40}$

as a blood-based biomarker for the diagnosis of CAA through a large-sample cohort study.

Conclusions

Given that differentiating CAA from AD is challenging because Aβ-PET tracers label both parenchymal and vascular Aβ,[23] our blood-based biosensor platform can help to diagnose CAA cost-effectively and non-invasively reducing the potential bias in the assessment of Aβ load. Additionally, our platform enables accurately and quickly screening of a small number of samples (within 30 min) with good sensitivity and realization in a portable size.

Author contributions

Hye Jin Kim: conceptualization; data curation; formal analysis; investigation; methodology; validation; visualization; writing – original draft. Dongsung Park: investigation; validation; writing – review & editing. Gyihyaon Yun: conceptualization; data curation; investigation; validation. Hongrae Kim: investigation; validation; writing – review & editing. Hyug-Gi Kim: data curation; writing – original draft; validation. Kyung Mi Lee: methodology; writing – original draft; validation. Il Ki Hong: methodology; writing – original draft; validation. Key-Chung Park: conceptualization; investigation; validation. Jin San Lee: conceptualization; data curation; investigation; methodology; supervision; validation; writing – original draft; writing – review & editing. Kyo Seon Hwang: conceptualization; data curation; methodology; project administration; resources; supervision; validation; writing – review & editing.

Conflicts of interest

There are no conflicts to declare.

Acknowledgements

This work was supported by the National Research Foundation of Korea (NRF) grant funded by the Korea government (Ministry of Science and ICT) [grant numbers NRF-2021R1A2C2004760, NRF-2021R1C1C1012429, and NRF-2021R1C1C2004400] and the Korea Health Industry Development Institute (KHIDI) [grant number. HU21C0053].

Notes and references

1 A. Charidimou, G. Boulouis, M. E. Gurol, C. Ayata, B. J. Bacskai, M. P. Frosch, A. Viswanathan and S. M. Greenberg, Emerging concepts in sporadic cerebral amyloid angiopathy, *Brain*, 2017, **140**, 1829–1850.

2 S. M. Greenberg, M. W. Vernooij, C. Cordonnier, A. Viswanathan, R. A. S. Salman, S. Warach, L. J. Launer, M. A. Van Buchem, M. M. Breteler and Microbleed Study Group, Cerebral microbleeds: a guide to detection and interpretation, *Lancet Neurol.*, 2009, **8**, 165–174.

3 M. M. Verbeek, B. P. Kremer, M. O. Rikkert, P. H. Van Domburg, M. E. Skehan and S. M. Greenberg, Cerebrospinal fluid amyloid β40 is decreased in cerebral amyloid angiopathy, *Ann. Neurol.*, 2009, **66**, 245–249.

4 D. Renard, G. Castelnovo, A. Wacongne, A. Le Floch, E. Thouvenot, J. Mas, A. Gabelle, P. Labauge and S. Lehmann, Interest of CSF biomarker analysis in possible cerebral amyloid angiopathy cases defined by the modified Boston criteria, *J. Neurol.*, 2012, **259**, 2429–2433.

5 M. Noguchi-Shinohara, J. Komatsu, M. Samuraki, I. Matsunari, T. Ikeda, K. Sakai, T. Hamaguchi, K. Ono, H. Nakamura and M. Yamada, Cerebral amyloid angiopathy-related microbleeds and cerebrospinal fluid biomarkers in Alzheimer's disease, *J. Alzheimer's Dis.*, 2017, **55**, 905–913.

6 G. Banerjee, R. Carare, C. Cordonnier, S. M. Greenberg, J. A. Schneider, E. E. Smith, M. Van Buchem, J. Van Der Grond, M. M. Verbeek and D. J. Werring, The increasing impact of cerebral amyloid angiopathy: essential new insights for clinical practice, *J. Neurol., Neurosurg. Psychiatry*, 2017, **88**, 982–994.

7 S. L. Risacher, N. Fandos, J. Romero, I. Sherriff, P. Pesini, A. J. Saykin and L. G. Apostolova, Plasma amyloid beta levels are associated with cerebral amyloid and tau deposition, *Alzheimer's Dement.: Diagn. Assess. Dis. Monit.*, 2019, **11**, 510–519.

8 H. J. Ahn, J. Chin, A. Park, B. H. Lee, M. K. Suh, S. W. Seo and D. L. Na, Seoul Neuropsychological Screening Battery-dementia version (SNSB-D): a useful tool for assessing and monitoring cognitive impairments in dementia patients, *J. Korean Med. Sci.*, 2010, **25**, 1071.

9 R. C. Petersen, Mild cognitive impairment as a diagnostic entity, *J. Intern. Med.*, 2004, **256**, 183–194.

10 S. W. Seo, S. S. Cho, A. Park, J. Chin and D. L. Na, Subcortical vascular versus amnestic mild cognitive impairment: comparison of cerebral glucose metabolism, *J. Neuroimaging*, 2009, **19**, 213–219.

11 H. J. Kim, J. Kim, Y. K. Yoo, J. H. Lee, J. H. Park and K. S. Hwang, Sensitivity improvement of an electrical sensor achieved by control of biomolecules based on the negative dielectrophoretic force, *Biosens. Bioelectron.*, 2016, **85**, 977–985.

12 H. J. Kim, D. Park, S. Y. Baek, S. H. Yang, Y. Kim, S. M. Lim, J. Kim and K. S. Hwang, Dielectrophoresis-based filtration effect and detection of amyloid beta in plasma for Alzheimer's disease diagnosis, *Biosens. Bioelectron.*, 2019, **128**, 166–175.

13 R. Pethig, Dielectric and electrical properties of biological materials, *J. Bioelectr.*, 1985, **4**, vii–ix.

14 G. McKhann, D. Drachman, M. Folstein, R. Katzman, D. Price and E. M. Stadlan, Clinical diagnosis of Alzheimer's disease: Report of the NINCDS-ADRDA Work Group* under the auspices of Department of Health and Human Services Task Force on Alzheimer's Disease, *Neurology*, 1984, **34**, 939–939.

15 A. Charidimou, J. Linn, M. W. Vernooij, C. Opherk, S. Akoudad, J. C. Baron, S. M. Greenberg, H. R. Jäger and D. J. Werring, Cortical superficial siderosis: detection and clinical significance in cerebral amyloid angiopathy and related conditions, *Brain*, 2015, **138**, 2126–2139.

16 H. Barthel, H. J. Gertz, S. Dresel, O. Peters, P. Bartenstein, K. Buerger, F. Hiemeyer, S. M. Wittemer-Rump, J. Seibyl, C. Reininger and O. Sabri, Cerebral amyloid-β PET with florbetaben (18F) in patients with Alzheimer's disease and healthy controls: a multicentre phase 2 diagnostic study, *Lancet Neurol.*, 2011, **10**, 424–435.

17 S. Bullich, J. Seibyl and A. M. Catafau, Optimized classification of $^{(18)}$F-Florbetaben PET scans as positive and negative using an SUVR quantitative approach and comparison to visual assessment, *Neuroimage Clin.*, 2017, **15**, 325–332.

18 M. Hernandez-Guillamon, P. Delgado, A. Penalba, D. Rodriguez-Luna, C. A. Molina, A. Rovira, J. Alvarez-Sabin, M. Boada and J. Montaner, Plasma β-amyloid levels in cerebral amyloid angiopathy-associated hemorrhagic stroke, *Neurodegener. Dis.*, 2012, **10**, 320–323.

19 K. Farid, A. Charidimou and J. C. Baron, Amyloid positron emission tomography in sporadic cerebral amyloid angiopathy: a systematic critical update, *Neuroimage Clin.*, 2017, **15**, 247–263.

20 A. Charidimou, K. Farid, H. H. Tsai, L. K. Tsai, R. F. Yen and J. C. Baron, Amyloid-PET burden and regional distribution in cerebral amyloid angiopathy: a systematic review and meta-analysis of biomarker performance, *J. Neurol., Neurosurg. Psychiatry*, 2018, **89**, 410–417.

21 E. Kövari, F. R. Herrmann, P. R. Hof and C. Bouras, The relationship between cerebral amyloid angiopathy and cortical microinfarcts in brain ageing and Alzheimer's disease, *Neuropathol. Appl. Neurobiol.*, 2013, **39**, 498–509.

22 J. Attems, Sporadic cerebral amyloid angiopathy: pathology, clinical implications, and possible pathomechanisms, *Acta Neuropathol.*, 2005, **110**, 345–359.

23 J. D. Goos, M. I. Kester, F. Barkhof, M. Klein, M. A. Blankenstein, P. Scheltens and W. M. van der Flier, Patients with Alzheimer disease with multiple microbleeds: relation with cerebrospinal fluid biomarkers and cognition, *Stroke*, 2009, **40**, 3455–3460.